INFLUENCE OF ESSENTIAL DIMENSIONS OF ROTOR GEOMETRY ON RELUCTANCE TORQUE GENERATION

Martin Pochyla
Doctoral Degree Programme (1), FEEC BUT
E-mail: xpochy01@stud.feec.vutbr.cz

Supervised by: Bohumil Klima
E-mail: klima@feec.vutbr.cz

ABSTRACT

The aim of this paper is to present example of FEM approach to determine suitable shape of reluctance rotor equipped with starting rotor cage, to produce the highest possible reluctance torque. The asynchronous start and further synchronous operation of the machine is requested. The research was performed with provided 4 pole squirrel cage induction motor with the nominal power of 240W. The influence of rotor dimensions on resulting reluctance torque is tested. The research was made based on finite element method calculation. The experimental verification of results has been performed on several rotor prototypes.

1. INTRODUCTION

The synchronous reluctant machines are simple, comparatively cheap and reliable devices that can be used in many applications. Current synchronous reluctance motors have been improved due to the technological evolution of the materials used in it is rotor. Many of the reluctance motors used in industry used to be fitted with cages in their rotors, similar to cages of induction motors mainly for starting purposes directly from the mains of power supply. In synchronous operation the cage serves as damper for the speed oscillations. The cage characteristics are important for the determination of the starting and running stability characteristics of the machine. [2]

The stator of synchronous and asynchronous motor has no difference in principle of operation. However, there is a significant difference in rotors of both machines. The very important parameter of reluctance rotor is so called “saliency ratio” represented by the ratio of rotor’s direct-axis inductance L_d and quadrature-axis L_q. For the proper operation of machine and to obtain the best possible output torque and power factor, it is necessary to achieve the highest possible saliency ratio. The output torque of machine is defined by following equation:

$$M = \frac{3}{4} p\left(L_d - L_q\right) i_s^2 \sin 2\kappa \qquad (1)$$

where p refers to number of pole-pairs, i_s to vector of stator current, and κ is the angle between stator current vector and rotor d-axis.

2. SELECTION OF ROTOR GEOMETRY

Various types of rotor constructions are available when designing a new rotor. One of the best saliency ratios can be offered with the axially laminated construction.[5] However, the rotor of provided induction motor is transversally laminated and contains a cage with 18 bars. Proposed shape of rotor is shown in Fig. 1.

Investigated geometry parameters of rotor were chosen with respect to the solution difficulty, available machine tools and also cost efficiency. Investigated parameters, that were stated as variables are illustrated in Fig 1. Consequently, the expected range of each parameter was determined (e.g. between 17° and 27° for parameter ***a***). In this range the step of parameter was chosen. For instance the step of parameter ***a*** is selected for 1°. With the help of AutoCAD software the geometries were created. These geometries were imported in FEM 4.0, where materials and boundary conditions were defined. After this procedure the LUA script was started.

3. CALCULATION PROCESS AND RESULTS

The aim of calculation is to find the parameter values, with the maximum reluctance torque and with respect to the minimum torque ripple. For the automatic calculation the LUA script was programmed. The script loads the geometry, performs the FEM magnetic field calculation and resulting torque estimation for all values of parameters. The torque is calculated during simulated synchronous operation of the machine in the range of mechanic 30 degrees. Because of synchronous operation simulation the κ was kept constant for all parameter values. The scheme of whole process is shown in Fig. 2.

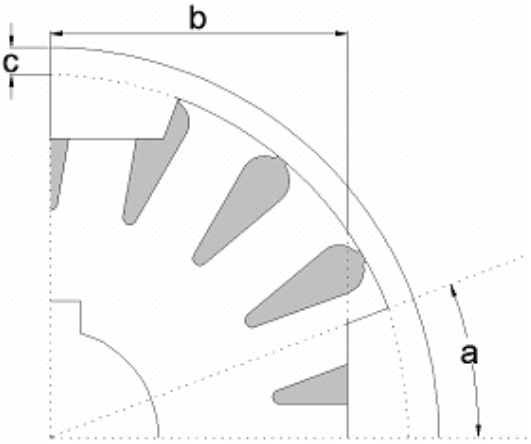

Fig. 1 Geometry dimensions suitable for the research of influence on resulting torque: ***a*** – cut out angle, ***b*** – cut out height, ***c*** - air-gap length

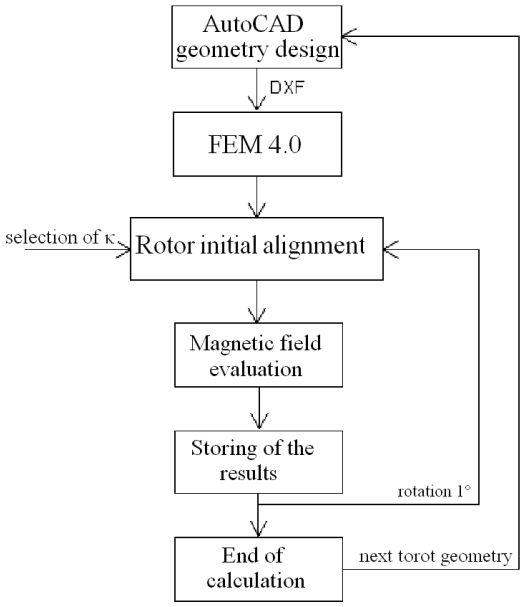

Fig. 2 Calculation process of torque progress according to chosen parameter of the rotor's geometry, where κ is the angle between the stator current vector and the d-axis of rotor

3.1. RESULTS FOR PARAMETER *A*

For different values of parameter ***a***, the various torque curves were obtained (see Fig. 3). Based on torque curves the maximal, minimal and average torque of each characteristic can be

specified. When plotted in graph, this values show the result. The importance of average torque is based on the fact, that rotor and stator slots causes torque ripples, and the resulting output torque of the motor is the average torque.

The results for parameter ***a*** (Fig. 4) show, that when increasing the salient pole (decrease of parameter ***a***), the d-axis inductance increases, however the q-axis inductance also increases slightly. When decreasing ***a*** further, the d-axis inductance stops to increase, but the q-axis inductance continues to increase. According to Fig. 4 this occurs approximately when ***a*** = 23°, where also the biggest torque ripple occurs. Therefore the optimal value of parameter ***a*** = 19° can be chosen. The decrease of average torque is not so significant and the torque ripple is considerably lower.

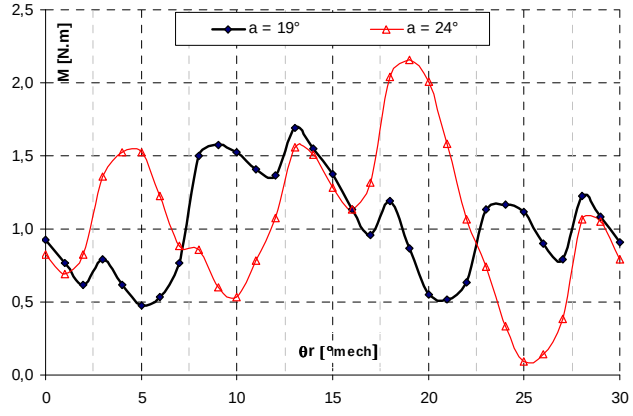

Fig. 3 Progress of calculated torque for rotors with ***a*** =19° and ***a*** = 24° when $\kappa = 7{,}5°$ mech is constant.

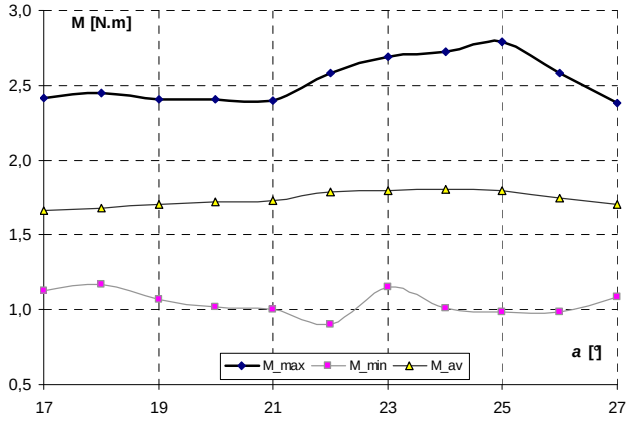

Fig. 4 Progress of minimal, average and maximum torque depending on the parameter ***a***, $\kappa = 7{,}5°$ mech is constant

3.2. RESULTS FOR OTHER PARAMETERS

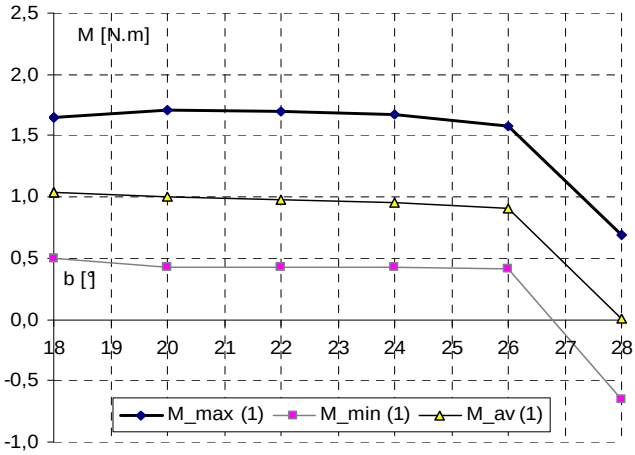

Fig. 5 Progress of minimal, average and maximum torque depending on the parameter ***b***, $\kappa = 7{,}5°$ mech = constant

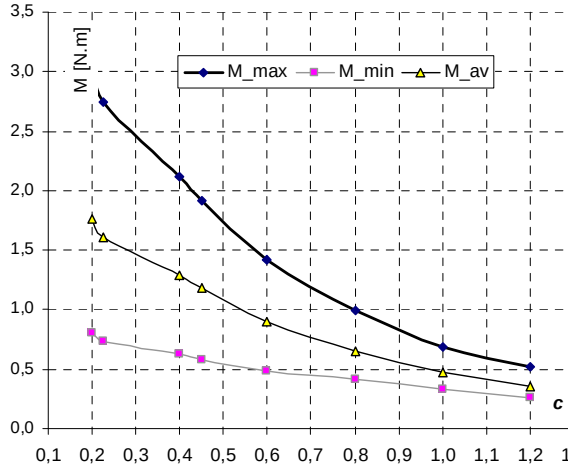

Fig. 6 Progress of minimal, average and maximum torque depending on the parameter ***c***, $\kappa = 7{,}5°$

The same process was undertaken for the resulting parameters ***b*** and ***c***. For parameter ***b*** it is obvious, that the smaller ***b***, the higher is the output torque. It is also obvious, that the smaller ***b***, **t**he lower is the mechanical strength of the rotor, and the more complicated is to manufac-

ture the rotor. So the selection is based on, the biggest possible value of ***b***, with the consideration that the torque does not decrease rapidly. (Fig. 5)

The air-gap length ***c*** has an enormous influence on the motor operation. As it can be seen in Fig 6, the higher air-gap is the lower torque is obtained. But what is important, the lower torque ripple occurs. The air-gap length has also serious influence on magnetization current and the power losses in the winding of the stator, as will be introduced in the following paragraph.

4. MAGNETIZING CURRENT AND AIR-GAP LENGTH

When calculating the linkage magnetic flux ψ of coil with N turns fed with current i, the Hopkin's law according to equation 2 can be used:

$$\psi = \frac{N^2 \cdot i}{R_m} \tag{2}$$

where R_m refers to a magnetic reluctance. Because the real motors are mostly fed from a voltage source, for the linkage magnetic flux the following formula can be applied:

$$\psi = \int u_i(t)dt + \psi_0 \tag{3}$$

This means, that the actual value of magnetic flux depends only on the integral of induced voltage, with no dependency on the current. Actually, the magnetic flux is forced to reach a certain level equal to the integral of the induced voltage and the current is only a result of this phenomena. In case, that the length of air-gap is increased, and the same voltage is applied, the magnetic flux remains constant. If the magnetic flux remains constant, the magnetizing current of machine must increase (considering that the number of turns remains constant according to formula 2).

Another important fact, that during the FEM calculation the pure sine wave current is inputted into the windings. When considering voltage fed motor, in ideal case we input pure sine wave voltage. Due to changing reluctance during rotation of the rotor, the non-sine wave current is withdrawn from network.

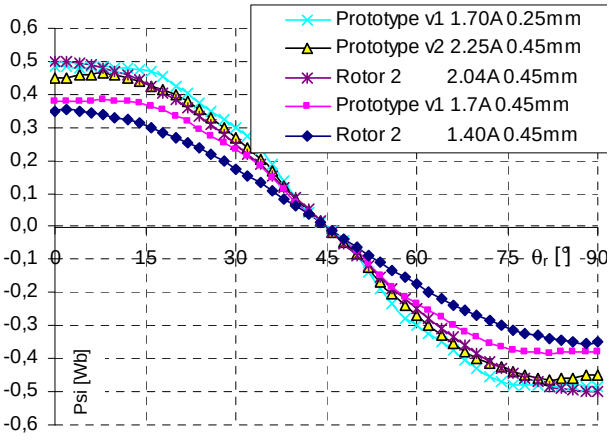

Fig. 7 Magnetic flux under various constrains as a function of rotor alignment, decreased magnetic flux of prototype v1 (longer airgap) and rotor 2 (lower input current)

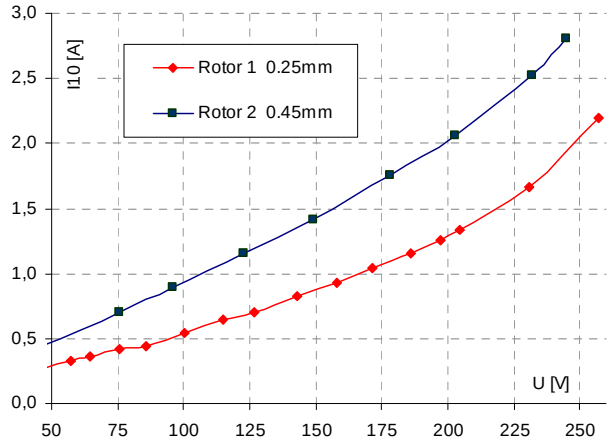

Fig. 8 Significant increase of the no-load current as a result of production discrepancy

On the other hand, when we input pure sine wave current, we are able to calculate a magnetic flux of each coil, and finally state a derivation of this flux, which in result gives us an induced voltage. If the induced voltage is calculated according to (3), the non-sine voltage progress is obtained as well.

The two shapes of rotors were manufactured and the measurements were performed. Due to production discrepancy the Rotor1 and derived protype v1 had smaller diameter when compared to Rotor2 and derived prototype v2. Consequently an experimental calculation was performed.

Experimental results are shown in Fig. 7. In case, that correct current related to the shape of rotor is used, the maximal flux remains approximately constant (0,5 Wb). In case that lower current or longer air-gap is used, the flux is approximately 0,1 Wb lower.

5. CONCLUSION

This paper demonstrates the FEM approach to determine optimal synchronous reluctance rotor geometry. After research several prototypes of reluctant rotors were manufactured. Because of production discrepancy, the longer air-gaps of the FEM optimized motor prototypes occurred, which decreased final efficiency and power factor of the machine. The output torque of the machine has been improved. According to formula (1), even higher reluctance torque can be achieved, if the air-gap would be smaller. This motor is capable of synchronous operation with asynchronous start without a frequency converter. The decrease of efficiency can be compensated with omitting the frequency converter. This solution is cheap and easy and fast to manufacture.

6. ACKNOWLEDGEMENT

The contribution is created under projects MSM 0021630516 and GA102/09/1875.

7. REFERENCES

[1] BOLDEA, Ion, NASAR, A. Syed. The induction machine handbook. [s.l.] : CRC Press, 2002. 500 s. ISBN 0-8493-0004-5.

[2] FERAZ, Carlos, SOUZA C.R., Reluctance synchronous motor asynchronous operation, Proceedings of the 2002 IEEE Canadian Conference on Electrical & Computer Engineering 0-7803-7514-9/02/$17.00

[3] HAATAJA, Jorma. A comparative performance study of four-pole induction motors and synchronous reluctance motors in variable speed drives. Lappeenranta, 2003. 138 s. Lappeenranta University of Technology. Dizertační práce. ISBN 951-764-772-7.

[4] MEEKER David, Finite Element Method Magnetics Version 4.0, User's Manual, 2004

[5] PEYMAN, Niazi, Permanent magnet assisted synchronous reluctance motor design and performance improvement, December 2005, 153 s., Texas A&M University, Dizertační práce